Thermal Sensitivity of Holey Fibers: a Numerical Analysis

R. Kotynski[a], T. Nasilowski[a], M. Antkowiak[a,b], F. Berghmans[a,b] and H. Thienpont[a]

[a]Department of Applied Physics and Photonics, Vrije Universiteit Brussel, Pleinlaan 2, B-1050, Brussels
[b]SCK.CEN, Boeretang 200, B-2400 Mol, Belgium

It is well known that holey fibers offer the possibility of obtaining high modal birefringence retaining single mode guidance at the same time. Such Hi-Bi holey fibers are of particular interest for sensing applications. We analyze the mechanisms contributing to the overall sensitivity of optical sensors based on holey fibers. For this purpose we investigate the shift of the Bragg-matched wavelength in a sensor with a Bragg grating as well as the change of birefringence in a polarimetric sensor.

Introduction

In air-silica microstructured fibers, also known as holey fibers, the large number of degrees of freedom encoded in the complex geometry of the cross-profile can be used to enhance or optimize most of the important fiber's specifications. This includes the possibility of tailoring the modal structure, the dispersion characteristics, or the mode area and following the strength of nonlinear effects. On the other hand, relatively little work so far has been devoted to asses the possibility of using holey fibers for sensing applications. From this point of view, especially interesting is the possibility of reaching a large value of modal birefringence [1-3], $B=\Delta n_{eff}$ while retaining single mode operation, as well as attaining the desired sensitivities. For the sake of simplicity, presently we address only the thermal responses of optical fiber sensors with a microstructured fiber. We analyze the response of a polarimetric sensor, given in terms of the thermal sensitivity dB/dT, as well as the response of a Bragg sensor, given in terms of the shift of the Bragg-matched wavelength $d\lambda_{Bragg}/dT$.

For air-silica fibers the thermally induced strain is negligible, since in these structures the thermal expansion is uniform. Therefore the temperature affects modal effective indices through the thermo-optic change of the refractive indices of silica glass and air, and through the thermal expansion of the fiber. The significance of the two effects is governed by the coefficient of thermal expansion $\alpha_{silica}=+5.5\cdot10^{-7}K^{-1}$ and the thermal coefficients $\beta_{silica}=+1.2\cdot10^{-5}K^{-1}$, $\beta_{air}=-0.9\cdot10^{-6}K^{-1}$ of the refractive indices for silica and air. We note the difference in their orders of magnitude, which roughly determine the contribution of the respective mechanisms to the sensor's thermal response, as well as the fact that in the classical Hi-Bi fibers, all the mentioned effects may be considered as corrections to the elasto-optic effect caused by thermally induced strain. As a consequence of the different physical mechanisms behind the response of holey fiber sensors, we expect them to feature novel sensitivity characteristics.

Numerical model for sensitivity calculation

As we already noticed, the change of the fiber's birefringence B with temperature T can be expressed using the contributions from thermal refractive index change and from thermal expansion. More precisely, we have [4]:

$$\frac{dB}{dT}=\frac{\partial B}{\partial l}\frac{\partial l}{\partial T}+\frac{\partial B}{\partial n_{silica}}\frac{\partial n_{silica}}{\partial T}+\frac{\partial B}{\partial n_{air}}\frac{\partial n_{air}}{\partial T}=\frac{\partial B}{\partial l}l\alpha_{silica}+\frac{\partial B}{\partial n_{silica}}\beta_{silica}+\frac{\partial B}{\partial n_{air}}\beta_{air}. \quad (1)$$

In a similar way, we may express the shift of a Bragg-matched wavelength in a Bragg grating based optical sensor. However this time, we need to include one more term corresponding to the longitudinal expansion of the grating:

$$\frac{d\lambda_{Bragg}}{dT}=\frac{d}{dT}(2n_{eff}\Lambda_{grating})=\lambda\alpha_{silica}+\frac{\lambda\beta_{silica}}{n_{eff}}\frac{\partial n_{eff}}{\partial n_{silica}}+\frac{\lambda\beta_{air}}{n_{eff}}\frac{\partial n_{eff}}{\partial n_{air}}+\frac{\lambda l\alpha_{silica}}{n_{eff}}\frac{\partial n_{eff}}{\partial l}. \quad (2)$$

In order to estimate the sensitivities we need to determine the modal indices differentiated over parameters appearing in the respective right hand terms of equations (1) and (2). For this purpose, we use a rigorous vectorial numerical model based on magnetic mode expansion in a trigonometric basis [5]. Our method can be considered as a variant of the plane-wave method, similar to [6-8]. The method implies periodic boundary conditions, in this context known as the supercell approximation.

Briefly, we solve the Maxwell's equations in the form of an eigen-equation for the transverse components of magnetic fields:

$$\left[\epsilon+\frac{1}{k^2}\nabla_t^2+\left(\frac{1}{k}\nabla_t\ln\epsilon\right)\times\frac{1}{k}\nabla_t\times\right]\boldsymbol{h}^{t,m}=(n_{eff}^m)^2\boldsymbol{h}^{t,m} \quad , \quad (3)$$

The dielectric index is assumed to be periodic over the area of the supercell spanned by the lattice vectors $\mathbf{a}_i$, and in consequence the magnetic fields preserve the same periodicity:

$$\epsilon(\boldsymbol{r})=\epsilon(\boldsymbol{r}+\boldsymbol{a}_i),\ \ \boldsymbol{h}^t(\boldsymbol{r})=\boldsymbol{h}^t(\boldsymbol{r}+\boldsymbol{a}_i),\ \ _{i=1,2} \quad , \quad (4)$$

For a hexagonal lattice and circular air holes a possible choice of the supercell is illustrated in Figure 1:

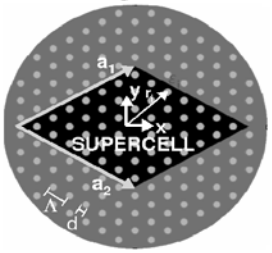

Fig.1 A typical choice for the definition of a supercell.

Following, we define the lattice inverse to the lattice spanned by the supercell:

$$\boldsymbol{a}_i\cdot\boldsymbol{b}_j=\delta_{i,j} \quad , \quad \boldsymbol{G}_l=l_1\cdot\boldsymbol{b}_1+l_2\cdot\boldsymbol{b}_2,\ \ l_i\in\mathbb{Z} \quad , \quad (5)$$

In the inverse lattice we introduce the set of plane-wave basis functions. The set is complete and orthonormal over the supercell.

$$\phi_l(\boldsymbol{r})=N\,e^{j\boldsymbol{G}_l\cdot\boldsymbol{r}},\ \ \langle\phi_l|\phi_m\rangle_{Supercell}=\delta_{l,m} \quad , \quad (6)$$

We expand the dielectric constant, its logarithm and the magnetic field components in the new basis:

$$\epsilon(\boldsymbol{r})=\sum_l \hat{\epsilon}_l\cdot\phi_l(\boldsymbol{r}) \ , \ln\epsilon(\boldsymbol{r})=\sum_l \hat{\kappa}_l\cdot\phi_l(\boldsymbol{r}) \ , \boldsymbol{h}^t(\boldsymbol{r})=\sum_l \begin{pmatrix}\widehat{h^x}_l\\ \widehat{h^x}_l\end{pmatrix}\phi_l(\boldsymbol{r}) \ , \tag{7}$$

Noting that the expansion coefficients for the dielectric index and its logarithm are given by respective Fourier transforms, for circular, elliptical, or polygonal holes we calculate these coefficients analytically. In the new basis, after its truncation, the eigen-equation for the magnetic modes becomes an algebraic eigen-problem:

$$\begin{bmatrix}L_{xx} & L_{xy}\\ L_{yx} & L_{yy}\end{bmatrix}\cdot\begin{bmatrix}\widehat{h^x}\\ \widehat{h^y}\end{bmatrix}=n_{eff}^2\begin{bmatrix}\widehat{h^x}\\ \widehat{h^y}\end{bmatrix} \ , \tag{8}$$

where the sub-matrices take the following form:

$$[L_{xx}]_{m,n}=\frac{\hat{\kappa}_{m-n}G_m^yG_{n-m}^y-\delta_{m,n}(G_m^{x\,2}+G_m^{y\,2})}{k^2}+\hat{\epsilon}_{m-n} \quad [L_{xy}]_{m,n}=\frac{-\hat{\kappa}_{m-n}G_m^xG_{n-m}^y}{k^2}$$
$$[L_{yy}]_{m,n}=\frac{\hat{\kappa}_{m-n}G_m^xG_{n-m}^x-\delta_{m,n}(G_m^{x\,2}+G_m^{y\,2})}{k^2}+\hat{\epsilon}_{m-n} \quad [L_{yx}]_{m,n}=\frac{-\hat{\kappa}_{m-n}G_m^yG_{n-m}^x}{k^2} \ . \tag{9}$$

We solve the matrix eigen-problem numerically, using Arnoldi's method, for eigenvalues in the vicinity of the squared refractive index of silica. In this way we find the modal indices together with the field distributions, and following, using formulas (1) and (2) we calculate the sensitivities of interest. In the numerical calculations we use over 5000 basis functions for the description of every field component, and twice more for the refractive index profile. For the supercell, we take 7x7 lattice elements. These values come from experience and should be considered as problem-dependent.

Thermal sensitivity of holey fibers

Now, we will calculate and discuss the thermal sensitivity characteristics for a particular highly birefringent microstructured fiber. In this example, we assume that the fiber is based on a hexagonal lattice, and birefringence is introduced by making the holes elliptical, which in turn breaks the usual C_{6v} symmetry and releases mode degeneracy.

We assumed that the wavelength is λ=1550nm, the pitch in the cladding is $\Lambda=\lambda/2$, and we varied the ellipticity of holes with the fill factor of air fixed at f=22.6%. In the selected range, the fiber has a single mode character. Figure 2 shows the temperature sensitivity of our polarimetric sensor, as well as of the Bragg sensor.

We note that the sensitivity has a positive value for a wide range of ellipticities, as opposed to the usual case of polarimetric fiber sensors. This result clearly indicates a difference in the physical mechanism behind sensing with holey fibers and is encouraging from the point of view of the possibility of getting novel sensing characteristics with holey fiber sensors. Moreover, there exists a threshold value for ellipticity, over which the sensitivity drops to negative values. The zero transition in between provides the possibility of making a sensor with ideal temperature compensation. Near that region, the main mechanism contributing to the overall sensitivity is the change of refractive index not of silica but of air. On the other hand, the response of a Bragg grating sensor given in terms of the relative shift of the Bragg-matched wavelength with respective contributions is typical to any other silica fiber,

and mainly depends on the thermo-optical effect in silica and longitudinal thermal expansion of the grating.

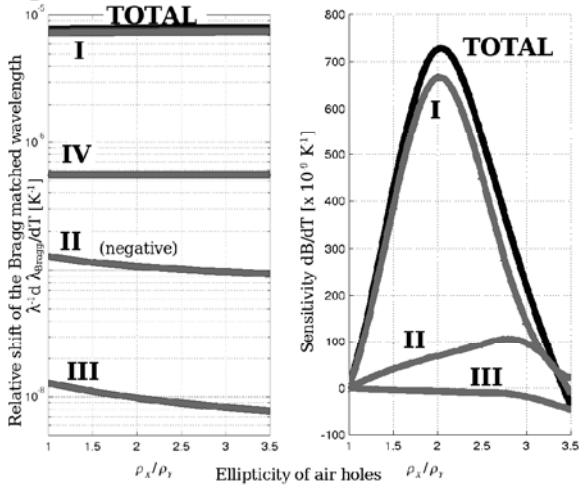

Fig.2 Thermal sensitivity of the holey fiber Bragg sensor (left), and polarimetric sensor (right) vs. hole ellipticity with the absolute values of contributions from I) thermo-optic effect in silica, II) thermo-optic effect in air III) fiber's cross-profile expansion, IV) fiber's longitudinal thermal expansion.

Conclusions

In the present paper we show that sensors with highly birefringent photonic crystal fibers feature novel sensitivity characteristics as a consequence of different physical mechanisms contributing to overall sensitivity. We analyzed the shift of the Bragg-matched wavelength in a sensor with a Bragg grating, as well as the change of birefringence in a polarimetric sensor. For the sake of simplicity we concentrated on the response of the sensor to temperature changes.

Acknowledgment

We acknowledge the funding from IAP Photon Network, FWO, GOA, and the OZR of the Vrije Universiteit Brussel.

References

[1] T. Hansen, J. Broeng, S. Libori, E. Knudsen, A. Bjarklev, J. R. Jensen, and H. Simonsen, "Highly birefringent index-guiding photonic crystal fibers," IEEE Phot.Techn.Lett. Vol.13, pp.588-590, 2001.

[2] D. Mogilevtsev, J. Broeng, S. E. Barkou and A. Bjarklev, "Design of polarization-preserving photonic crystal fibers with elliptical pores," J. Opt. A: Pure Appl. Opt. vol. 3, pp. 141-143, 2001.

[3] A. Ortigosa-Blanch, J. Knight, W. Wadsworth, J. Arriaga, B. Mangan, T. Birks, and P. Russel, "Highly birefringent photonic crystal fibers," Opt. Lett. Vol. 25, 1325-1327, 2000.

[4] R. Kotynski, T. Nasilowski, M. Antkowiak, F. Berghmans, and H. Thienpont, Sensitivity of Holey Fiber Based Sensors, in Proc. of the 2nd European Symposium on Photonic Crystals ICTON 2003, Warsaw, 340-343, 2003.

[5] R. Kotynski, T. Nasilowski, and H. Thienpont, "Vectorial mode characterization of microstructured optical fibers," Proc. of the Annual Symposium of the IEEE/LEOS Benelux Chapter, 187-190, 2002.

[6] Z. Zhu, and T.G. Brown, Analysis of the space filling modes of photonic crystal fibers, Opt. Express. vol. 8, pp. 547-554, 2001.

[7] M. Szpulak, T. Martynkien, and W. Urbanczyk, Birefringent Photonic Crystal Holey Fibers Based on Hexagonal Lattice, in Proc. of the 2nd European Symposium on Photonic Crystals ICTON 2003, Warsaw, 333-336, 2003.

[8] A. Ferrando, J.J. Miret, E. Silvestre, P. Andres, M. V. Andres, "Full-vector analyses of a realistic photonic crystal fibre," Opt. Lett. vol. 24, pp. 276-277, 1999.